Available online at www.sciencedirect.com

ScienceDirect

IFAC Papers Online CONFERENCE PAPER ARCHIVE

IFAC PapersOnLine 51-24 (2018) 52–59

Adaptive Signal Processing Strategy for a Wind Farm System Fault Accommodation ⋆

Silvio Simani * **Paolo Castaldi** **

* *Department of Engineering, University of Ferrara, Ferrara (FE) 44122 Italy (e–mail: silvio.simani@unife.it).*

** *Department of Electrical, Electronic and Information Engineering (DEI), University of Bologna, Bologna (BO) 40126 Italy (e–mail: paolo.castaldi@unibo.it)*

Abstract: In order to improve the availability of offshore wind farms, thus avoiding unplanned operation and maintenance costs, which can be high for offshore installations, the accommodation of faults in their earlier occurrence is fundamental. This paper addresses the design of an active fault tolerant control scheme that is applied to a wind park benchmark of nine wind turbines, based on their nonlinear models, as well as the wind and interactions between the wind turbines in the wind farm. Note that, due to the structure of the system and its control strategy, it can be considered as a fault tolerant cooperative control problem of an autonomous plant. The controller accommodation scheme provides the on–line estimate of the fault signals generated by nonlinear filters exploiting the nonlinear geometric approach to obtain estimates decoupled from both model uncertainty and the interactions among the turbines. This paper proposes also a data–driven approach to provide these disturbance terms in analytical forms, which are subsequently used for designing the nonlinear filters for fault estimation. This feature of the work, followed by the simpler solution relying on a data–driven approach, can represent the key point when on–line implementations are considered for a viable application of the proposed scheme.

Keywords: Offshore wind farm, fault diagnosis, fault tolerant control, data–driven method, model–based approach, adaptive control, nonlinear control.

1. INTRODUCTION

In general, wind turbines in the megawatt size are expensive, and hence their availability and reliability must be high in order to maximise the energy production. This issue could be particurarly important for offshore installations, where Operation and Maintenance (O & M) services have to be minimised, since they represent one of the main factors of the energy cost. The capital cost, as well as the wind turbine foundation and installation determine the basic term in the cost of the produced energy, which constitute the energy 'fixed cost'. The O & M represent a 'variable cost' that can increase the energy cost up to about the 30%. At the same time, industrial systems have become more complex and expensive, with less tolerance for performance degradation, productivity decrease and safety hazards. This leads also to an ever increasing requirement on reliability and safety of control systems subjected to process abnormalities and component faults. As a result, it is extremely important the Fault Detection and Diagnosis (FDD) or the Fault Detection and Isolation (FDI) tasks, as well as the achievement of fault–tolerant features for minimising possible performance degradation and avoiding dangerous situations. With the advent of computerised control, communication networks and information techniques, it makes possible to develop effective real–time monitoring and fault–tolerant design techniques for industrial processes, but brings challenges (Simani and Farsoni (2018)). This work aims at providing the development of a fault tolerant control (FTC) scheme with application to a wind farm simulator (Odgaard and Stoustrup (2013)).

In the last years, many works have been proposed on wind turbine FDI/FDD, and the most relevant are recalled *e.g.* in (Simani and Farsoni (2018)). On the other hand, regarding the FTC problem for wind turbines, it was analysed with reference to an offshore wind turbine benchmark (Simani and Farsoni (2018)). In general, FTC methods are classified into two types, *i.e.* Passive Fault Tolerant Control Scheme (PFTCS) and Active Fault Tolerant Control Scheme (AFTCS) (Simani and Farsoni (2018)). In PFTCS, controllers are fixed and are designed to be robust against a class of presumed faults. In contrast to PFTCS, AFTCS react to the system component failures actively by reconfiguring control actions so that the stability and acceptable performance of the entire system can be maintained. In particular for the wind farm benchmark considered in this paper, FTC designs were also addressed in (Odgaard and Stoustrup (2013)). These processes are complex nonlinear dynamic systems, whose aerodynamics are nonlinear and unsteady, whilst their rotors are subject to complicated turbulent wind inflow fields driving fatigue loading. Therefore, the control of wind turbines and wind

⋆ Paper partially supported by FAR2017 local fund by the University of Ferrara, Italy.

10.1016/j.ifacol.2018.09.528

farms represents a complex and challenging task (Simani and Castaldi (2018)).

In more detail, this paper addresses the development of an AFTCS, that integrates a robust fault estimation scheme with the design of a controller accommodation system. In particular, the methodology for the on–line fault estimation relies on adaptive filters designed via the NonLinear Geometric Approach (NLGA). The controller accommodation scheme exploiting a second control loop depends on the on–line estimate of the fault signal itself. The suggested nonlinear fault reconstructors exploit the same approach described in (Simani and Castaldi (2014)), which was applied to a single wind turbine. Moreover, this paper proposes the design of nonlinear filters that are decoupled from both the disturbance and the interactions of the wind turbines of the wind farm. This method allows also to deal with possible internal feedbacks and their effects that additionally main influence the final performance.

In this way, the issue considered in this paper can be considered as fault tolerant cooperative control problem of an autonomous process. Therefore, under this consideration, and the regulation requirements, a Fault Tolerant Cooperative Control (FTCC) solution can be exploited to improve the safety and reliability, and guarantee graceful degradation of the working conditions due to faults affecting the process under investigation. The FTCC investigation have been just initiated recently, and some challenging issues require further investigation. In particular, with reference to the considered multiple wind turbine system, actuators are physical devices that convey energy into the system, both by altering its maneuvers and attenuating the effects of disturbances. To be more specific, the actuators of the wind turbines work collectively to maintain a prescribed power generation. Therefore, actuator faults have to be considered in a cooperative manner. On the other hand, the capability of the whole wind farm needs to be explicitly considered when designing the FTCC scheme, such that the control reallocation for each wind turbine of the park is achievable and feasible. This work will present a possible solution to the FTCC problem, when the offshore wind park is considered as an autonomous system, which should maintain prescribed performance even if malfunctions may occur. The proposed solution includes the development of a fault diagnosis module, which is integrated into a FTC scheme, and its verification on the benchmark simulator.

The nonlinear fault estimation procedure is based on the NLGA scheme also exploited in (Simani and Castaldi (2014)). Moreover, the direct application of the suggested methodology, or any other schemes relying on *analytical* disturbance decoupling, is almost impossible, due to the benchmark model structure. In fact, the wind turbine aerodynamic description depends on a mapping to the power conversion ratio from tip–speed ratio and blade pitch angles. This mapping is not known in any analytical form, but is represented by an approximated two–dimensional map. Thus, this paper suggests to estimate this power conversion ratio in an analytical form as two–dimensional polynomial. This relation is subsequently used for designing the disturbance decoupled fault estimation module. The same estimation procedure is applied for deriving the analytical description of the wake model representing the interactions among the different wind turbines of the wind park, which represents the original contribution of this paper. These interactions are considered as a disturbance term, since, together with the wind model, they limit the performances of the FTC scheme. Note that different FDI/FDD approaches, which highlighted the main features of the wind farm, were applied to the same wind farm challenge and summarised in (Simani and Farsoni (2018)).

Both the adaptive filters and the AFTCS are analysed with respect to the wind park benchmark described in (Odgaard and Stoustrup (2013)), in the presence of faults, disturbances, measurement noise, and modelling errors. Note that a similar AFTCS applied to the same benchmark but exploiting fuzzy filters is also described in (Simani et al. (2018)). Therefore, the design of the overall AFTCS for the wind park simulator and based on nonlinear filters represents the novel contribution of this paper. The proposed solution will be also compared with respect to some solutions presented in (Simani and Farsoni (2018)). On one hand, the method proposed in this paper is based on adaptive filters that try to counteract on–line any fault occurrences. On the other hand, the solution using fuzzy filters is designed off–line to passively tolerate all the possible faults affecting the controlled system, thus representing a PFTCS. It is worth noting also that, for the first time, the presented disturbance decoupling problem has been solved for the considered wind farm benchmark. This represents another important contribution of the work. Note that this paper extends the methods addressed in (Simani and Castaldi (2017)) and compares the results already presented in (Simani and Castaldi (2018)).

Finally, the work is organised as follows. Section 2 recalls the wind park simulator. Section 3 describes the fault estimation scheme, followed by the development of the structure of the AFTCS. The achieved results are reported in Section 4. Comparisons with different FTC strategies are also reported. Finally, Section 5 concludes the paper by summarising the main achievements of the work, and providing some suggestions for further research topics.

2. WIND FARM BENCHMARK

This benchmark challenge represents a wind farm with 9 wind turbines arranged in a square grid layout (Odgaard and Stoustrup (2013)). The distance between the wind turbines in both directions are 7 times the rotor diameter, L. Two measuring masts are located in front of the wind turbines, one in each of the wind directions considered in this benchmark model, *i.e.* 0^o and 45^o. The wind speed is measured by these measuring masts and they are located in a distance of 10 times L in front of the wind farm. The wind turbines of the farm are defined in a coordinate system as illustrated in (Odgaard and Stoustrup (2013)). The farm uses the generic 4.8MW wind turbine considered in (Simani and Farsoni (2018)). The turbine is a three bladed horizontal axis, pitch controlled variable speed wind turbine. Each of the wind turbines are described by simplified models including control logics, variable parameters and three states. The i–th wind turbine model generates the electrical power, $P_{i\,g}(t)$, the collective pitch angle, $\beta_i(t)$, and the generator speed, $\omega_{i\,g}(t)$. Note that

only one measured pitch angle is provided since it is assumed that the wind turbine controller regulates the pitch angles in the same way. The two scenarios with different wind directions but driven both by the same wind speed sequence $v_w(t)$ (possibly with a time shift) are considered. The wind sequence contains a wind mean speed increasing from 5 m/s to 15 m/s, and with a peak value of about 23 m/s. In this benchmark model a very simple wind farm controller is used, which provides the wind turbine controllers with a power reference $P_{i\,ref}(t)$. If the wind farm is requested to generate a power lower than the available one, the references are evenly distributed among the wind turbine controllers. It is worth noting that the wind farm considered here could be seen as simplistic model. However, the simulator can fit actual wind farm installation with good accuracy as analysed in detail in (Simani and Farsoni (2018)). However, more detailed wind farm model, which is beyond the scope of this work, can be found *e.g.* in (Simani and Farsoni (2018)).

An important issue not considered in (Simani and Castaldi (2018, 2017)) and possibly limiting the achievable performances of the FTC design, is represented by the interactions and internal feedback among the wind turbines, which can mask the effects of the faults affecting the wind turbines themselves, as described in the following. The wind farm model consists of three parts depicted in Fig. 1.

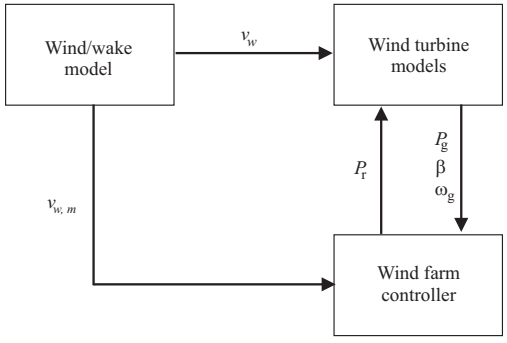

Fig. 1. The general wind farm model structure.

In particular, the wake model will be recalled below (Odgaard and Stoustrup (2013)). This model represents the wind distribution in the farm, and thereby also describes the interconnections between the wind turbines through the wakes. These wakes depends on how the wind turbines are controlled, so an upwind turbine can either increase or decrease the wake at the downwind turbine by the control actions. However, in order to keep the benchmark model simple, it is assumed that the wakes are independent of the control of the individual wind turbines. In the model sketched in Fig. 1, v_w represents the vector of the wind speeds, $v_{i,\,w}$, whilst $v_{w,\,m}$ is the vector of the measured wind speeds at the measuring masts, $v_{i,\,w,\,m}$. P_r is the vector of the power references to the wind turbines, $P_{i\,r}$, and P_g is the vector of the generated electrical powers for the i–th wind turbine, $P_{i\,g}$. β is the vector of the pitch angle for each wind turbine, β_i, whilst ω_g is the vector of the generator speed of the wind turbines, $\omega_{i\,g}$.

The wind farm is driven by a wind sequence rather than a stochastically generated signal, since it has to describe the entire operation range of the wind turbines, which is challenging. The wind sequence is delayed by the distance between the different points in the wind farm (measuring masts and wind turbines) and the mean wind speed. The distances depend on the wind direction considered in the benchmark (Odgaard and Stoustrup (2013)). The wake is modelled by a wind deficit between the wind turbines by a factor of 0.9. The turbulence of the wind is modelled in this model by random noise with a variance of 0.2.

Regarding the two remaining blocks of Fig. 1, the wind turbine models are relatively simple, whose implementation is described in (Simani and Farsoni (2018)). Each wind turbine model consists of three subsystems: a power model, a pitch model, and a generator speed model. On the other hand, the wind farm implements a quite simple controller. It provides the wind turbine controllers with a power reference. In case that the wind farm is requested to lower the generated power below the available power, references are evenly distributed to the wind turbine controllers.

With these assumptions, the complete continuous–time description of the wind farm under diagnosis has the following form:

$$\begin{cases} \dot{x}_c(t) = f_c\left(x_c(t), u(t)\right) \\ y(t) = x_c(t) \end{cases} \tag{1}$$

where $u(t) = [v_{i\,w}(t),\, v_{j\,w\,m}(t),\, P_{i\,r},\, \beta_i(t)]^T$ and $y(t) = x_c(t) = [\omega_{i\,g}(t),\, P_{i\,g}(t)]^T$ are the input and the monitored output measurements, respectively. The subscript i indicates the i–th wind turbine of the wind farm possibly affected by the j–th wind wake ($i,\, j = 1, \ldots, 9$, with $i \neq j$). $f_c(\cdot)$ represents the continuous–time nonlinear function, which will be used for acquiring the N sampled data $u(k)$ and $y(k)$, with $k = 1,\, 2,\, \ldots\, N$. This representation allows to include uncertain terms, mutual interactions and internal feedback affecting the overall process under investigation. In fact, it contains also the descriptions of the disturbance terms related to the wind speed $v_w(t)$ via the nonlinear aerodynamic effect and the wind wakes $v_{w,m}$ due to the wind turbine interactions, which will be estimated as presented in Sections 3 and 4.

In this benchmark three faults are considered that influence the measured variables from the wind turbine, *i.e.* $\beta_i(t)$, $\omega_{i\,g}(t)$, and $P_{i\,g}(t)$. It is also assumed that the considered faults can be detected at a wind farm level by comparing the performance from other wind turbines in the wind farm, but they are difficult to detect at a wind turbine level. Moreover, these three faults affect different wind turbines at different times, as described in more detail in (Odgaard and Stoustrup (2013)).

In the following, the relations among the fault cases considered here and the wind turbines of the wind park have been described. It will be shown that the disturbance decoupling approach described in Section 3 enhances the FDD task, which is exploited for controller accommodation purpose, thus representing the key point of the contribution. In particular, Table 1 shows the fault distribution among the wind turbines, in the case of single fault occurrence.

The fault 1 represents the debris build–up, due *e.g.* to dirt on the wind turbine blades, which changes the aerodynamics of the wind turbine, typically by lowering the maximally achievable power. On the other hand, the fault

Table 1. Faults affecting the wind turbines of the wind park benchmark.

Fault affecting the wind turbine nr.	Fault case
$i = 2$ & $i = 7$	Fault 1
$i = 1$ & $i = 5$	Fault 2
$i = 6$ & $i = 8$	Fault 3

2 is due to a misalignment of one or more blades originated during the installation of the wind turbine. This leads to an offset between the measured and actual pitch angle for one or more blades, thus introducing a difference between the blade loads, for the different blades at the same rotational position, which can excite structural modes. Finally, the fault 3 describes a change in the drive train damping due to wear and tear. Note that this fault is currently diagnosed by applying condition monitoring techniques to the drive train in order to detect changes in the frequency spectra of different vibration measurements. It is clearly important to investigate if the same result can be obtained using the the measurements available in the control systems either on wind turbine or wind farm level. In (Simani and Farsoni (2018)) a number of contributions on the wind turbine FDI problem were analysed, and it was concluded that the model–based FDI solutions are not suitable for detecting this fault type. More details on these faults can be found in (Simani and Farsoni (2018)).

The remainder of this section describes the relations among the fault cases considered above and the monitored measurements acquired from the wind park benchmark and reported in Fig. 1, in the presence of uncertainty and measurement errors. In fact, Section 4 will show that the design of the nonlinear filters for fault estimation is enhanced using the methodology proposed in this work, thus representing one of the main motivations of the suggested approach. In particular, Table 2 shows the effects of the considered fault cases with respect to the acquired input and output measurements of the wind park simulator. These measurements feeding the model (1) will be exploited for the design of the nonlinear filters described in Sections 3 and 4.

Table 2. Fault sensitivity for the wind park benchmark.

Variable	Measurements	Fault
u	$v_{2\,w}$, $v_{7\,w}$, $v_{4\,w\,m}$, $v_{9\,w\,m}$, $P_{2\,r}$, β_7	Case 1
y	$\omega_{9\,g}$, $P_{4\,g}$	
u	$v_{1\,w}$, $v_{5\,w}$, $v_{2\,w\,m}$, $v_{6\,w\,m}$, $P_{1\,r}$, β_2	Case 2
y	$\omega_{5\,g}$, $P_{6\,g}$	
u	$v_{6\,w}$, $v_{8\,w}$, $v_{3\,w\,m}$, $v_{7\,w\,m}$, $P_{6\,r}$, β_3	Case 3
y	$\omega_{8\,g}$, $P_{7\,g}$	

Table 2 was obtained by performing a fault sensitivity analysis (Simani and Farsoni (2018)). In practice, Table 2 is thus built by selecting the most sensitive measurements of (1) with respect to the simulated fault conditions. Obviously, when different fault conditions have been considered with respect to the scenario of this work, different measurements should probably be taken into account. Moreover, faults different from the ones proposed in (Odgaard and Stoustrup (2013)) could have different effects on the considered measurements. On the other hand, the fault sensitivity depends on the fault itself and the affected wind turbine. These issues could require further investigations, as suggested in (Simani and Farsoni (2018)).

3. NONLINEAR FAULT DIAGNOSIS AND COMPENSATION

The proposed AFTCS consists of three phases. The first step regards the estimation of the nonlinear disturbance distribution functions, which are required for the design of the NLGA adaptive filter for fault estimation. The fault reconstruction is thus exploited by the control scheme for compensating the alterations of both the measured and control signals.

3.1 Disturbance Function Estimation

In order to achieve an effective and robust FTC solution, the disturbances acting on the system have to be decoupled. Section 2 highlighted that these disturbances are represented by two effects. The first one derives from the wind signal $v_{i\,w}$ affecting the i–th wind turbine model of the wind farm through its power coefficient C_p. The decoupling of this effect was already investigated in (Simani and Castaldi (2014)) but applied to a single wind turbine. It will be used here and applied to the different models of the wind farm. The second disturbance effect is due to the interactions among the wind turbines, and represented by the signals $v_{j\,w\,m}(t)$ of the wind wakes.

Solutions dealing with the first disturbance term were based on the estimation of both the C_p values and the wind speed $v_w(t)$, as described *e.g.* in (Odgaard and Stoustrup (2012)). Regarding the wind wakes, a novel strategy based on the NLGA scheme is proposed here. In particular, as for the decoupling of the wind speed $v_w(t)$ addressed in (Simani and Castaldi (2014)), this approach requires the analytical knowledge of the nonlinear disturbance distribution relation of the unknown inputs $v_{j\,w\,m}(t)$. In more detail, as shown in (Simani and Castaldi (2014)), the $C_p\,(\beta,\,\lambda)$–map appearing in the wind turbine aerodynamic models was estimated by means of a two–dimensional polynomial representation, which was a function of the tip–speed ratio λ and the blade pitch angles β. The same approach was exploited for decoupling the further inputs $v_{j\,w\,m}(t)$ by following the data–driven estimation procedure recalled in (Simani and Castaldi (2014)).

3.2 Adaptive Fault Estimator Design

Once the disturbance description has been obtained in analytical form, the second stage of the AFTCS design is based on the development of the nonlinear FDD filters. Their structure is obtained by exploiting a disturbance decoupling scheme belonging to the NLGA framework (Simani and Castaldi (2014)). A coordinate transformation, highlighting a subsystem affected by the fault and decoupled by the disturbances, is the starting point to design adaptive filters for fault estimation. It is worth observing that, by means of this NLGA approach, the fault estimate is decoupled from the disturbance d, which in this work are represented by the vector $[v_{i\,w},\, v_{j\,w\,m}]$.

The proposed approach is applied to the general nonlinear model in the form (2):

$$\begin{cases} \dot{x} = n(x) + g(x)\, c + \ell(x)\, f + p_d(x)\, d \\ y = h(x) \end{cases} \quad (2)$$

where the state vector $x \in \mathcal{X}$ (an open subset of $\mathbb{R}^{\ell_n}$), $c(t) \in \mathbb{R}^{\ell_c}$ is the control input vector, $f(t) \in \mathbb{R}$ is the fault, $d(t) \in \mathbb{R}^{\ell_d}$ is the disturbance vector, and $y \in \mathbb{R}^{\ell_m}$ is the output vector. $n(x)$, $\ell(x)$, the columns of $g(x)$, and $p_d(x)$ are smooth vector fields, with $h(x)$ a smooth map.

The development of the NLGA strategy for the design of the estimator for the fault f with the decoupling of the disturbance d is based on the procedure presented in (Castaldi et al. (2010)). It was shown that the considered NLGA scheme extended to the fault diagnosis problem is based on a coordinate change in the state space and in the output space, such that, by using the new (local) state and output coordinates $(\bar{x}, \bar{y})$, the system (2) is transformed into:

$$\begin{cases} \dot{\bar{x}}_1 = n_1(\bar{x}_1, \bar{x}_2) + g_1(\bar{x}_1, \bar{x}_2)\, c + \ell_1(\bar{x}_1, \bar{x}_2, \bar{x}_3)\, f \\ \dot{\bar{x}}_2 = n_2(\bar{x}_1, \bar{x}_2, \bar{x}_3) + g_2(\bar{x}_1, \bar{x}_2, \bar{x}_3)\, c + \\ \quad + \ell_2(\bar{x}_1, \bar{x}_2, \bar{x}_3)\, f + p_2(\bar{x}_1, \bar{x}_2, \bar{x}_3)\, d \\ \dot{\bar{x}}_3 = n_3(\bar{x}_1, \bar{x}_2, \bar{x}_3) + g_3(\bar{x}_1, \bar{x}_2, \bar{x}_3)\, c + \\ \quad + \ell_3(\bar{x}_1, \bar{x}_2, \bar{x}_3)\, f + p_3(\bar{x}_1, \bar{x}_2, \bar{x}_3)\, d \\ \bar{y}_1 = h(\bar{x}_1) \\ \bar{y}_2 = \bar{x}_2 \end{cases} \quad (3)$$

with $\ell_1(\bar{x}_1, \bar{x}_2, \bar{x}_3)$ not identically zero. As remarked in (Castaldi et al. (2010)), this procedure yields to the observable subsystem (3) which, if it exists, is affected by the faults f, and not affected by disturbances d.

This transformation can be applied to the system (2), if and only if some fault detectability conditions are satisfied (Castaldi et al. (2010)). The system (2) in the new reference frame is decomposed into three subsystems (3), where the first one (the so–called $\bar{x}_1$–subsystem) is always decoupled from the disturbances d and affected by the faults f, as described by (4):

$$\begin{cases} \dot{\bar{x}}_1 = n_1(\bar{x}_1, \bar{y}_2) + g_1(\bar{x}_1, \bar{y}_2)\, c + \ell_1(\bar{x}_1, \bar{y}_2, \bar{x}_3)\, f \\ \bar{y}_1 = h(\bar{x}_1) \end{cases} \quad (4)$$

where, as the state $\bar{x}_2$ in (3) is assumed to be measured, the variable $\bar{x}_2$ in (4) is considered as independent input, and denoted with $\bar{y}_2$.

The proposed NLGA adaptive filter is based on the least–squares algorithm with forgetting factor proposed in (Castaldi et al. (2010)), and it is described by the adaptation law (5):

$$\begin{cases} \dot{P} = \beta\, P - \dfrac{1}{N^2} P^2 \breve{M}_1^2, & P(0) = P_0 > 0 \\ \dot{\hat{f}} = P\, \epsilon\, \breve{M}_1, & \hat{f}(0) = 0 \end{cases} \quad (5)$$

with (6) representing the output estimation, and the corresponding normalised estimation error:

$$\begin{cases} \hat{\breve{y}}_{1s} = \breve{M}_1\, \hat{f} + \breve{M}_2 + \lambda\, \breve{\bar{y}}_{1s} \\ \epsilon = \dfrac{1}{N^2} \left(\bar{y}_{1s} - \hat{\breve{y}}_{1s} \right) \end{cases} \quad (6)$$

where all the involved variables of the adaptive filter are scalar. In particular, $\lambda > 0$ is a parameter related to the bandwidth of the filter, $\beta \geq 0$ is the forgetting factor, and $N^2 = 1 + \breve{M}_1^2$ is the normalisation factor of the least–squares algorithm. Moreover, the proposed adaptive filter adopts the signals $\breve{M}_1$, $\breve{M}_2$, $\breve{\bar{y}}_{1s}$ which are obtained by means of a low–pass filtering of the signals M_1, M_2, $\bar{y}_{1s}$ as follows:

$$\begin{cases} \dot{\breve{M}}_1 = -\lambda\, \breve{M}_1 + M_1, & \breve{M}_1(0) = 0 \\ \dot{\breve{M}}_2 = -\lambda\, \breve{M}_2 + M_2, & \breve{M}_2(0) = 0 \\ \dot{\breve{\bar{y}}}_{1s} = -\lambda\, \breve{\bar{y}}_{1s} + \bar{y}_{1s}, & \breve{\bar{y}}_{1s}(0) = 0 \end{cases} \quad (7)$$

The considered adaptive filter is described by the systems (5), (6), and (7). It is worth noting that in (Castaldi et al. (2010)) it was showed that this adaptive filter provides an estimation $\hat{f}(t)$ that asymptotically converges to the magnitude of the actual fault f. The reconstructed faults can be represented by general models, as described in (Castaldi et al. (2017)). Note also that the approach was extended to the sensor fault estimation by means of the so–called sensor fault signature, as shown in (Baldi et al. (2018)).

3.3 Active Fault Tolerant Control Scheme

Once the robust FDD module has been obtained, the fault estimations are used for the compensation of the signals P_g, β, and ω_g exploited by the wind farm controller of Fig. 1. This phase represents the third step of the AFTCS development. In particular, in order to compute the simulation results described in Section 4, the AFTCS scheme has been completed by means of the wind farm controller described in (Odgaard and Stoustrup (2013)), as shown in Fig. 2.

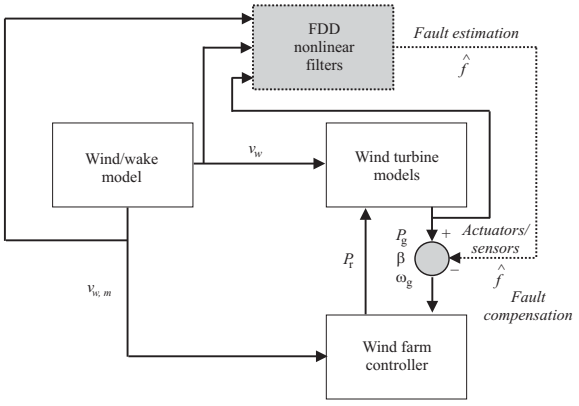

Fig. 2. Scheme of the integrated AFTCS.

The scheme depicted in Fig. 2 shows that the AFTCS strategy is implemented by integrating the fault estimator module with the existing control system. From the controlled input and output signals, the fault estimation module provides the correct estimation of the faults f, which are injected into the control loops, in order to compensate the effect of the faults themselves. After these corrections, the wind turbine controller provides the nominal tracking of the reference signal.

Finally, it is worth noting that, in steady–state conditions, when the fault effect is completely eliminated, the performances of the AFTCS are the same of the fault–free situation. The stability properties of the AFTCS should be considered only in transient conditions, when the fault is not compensated. In fact, in these conditions, the fault

estimation error corresponds to a signal injected into the feedback loop of Fig. 2. It is possible to show that the fault estimation error is limited and convergent to zero, thus the stability of the complete system is maintained, by following *e.g.* the procedure developed in (Simani and Castaldi (2014)).

4. SIMULATION RESULTS

This section describes the design and the simulations of the AFTCS applied to the wind park benchmark. In particular, the results achieved from the estimation of the disturbance terms appearing in (2) are firstly summarised. Once the disturbance decoupling has been achieved, the performances of the AFTCS method are reported.

In more detail, the C_p–map entering into the aerodynamic model of the wind turbines has been approximated by using the two–dimensional polynomial in the form (8):

$$\hat{C}_p\,(\lambda,\,\beta) = 0.010\,\lambda_i^2 + 0.0003\,\lambda_i^3\,\beta_i - 0.0013\,\lambda_i^3 \qquad (8)$$

for the i–th turbine of the wind park. More details they can be found in (Simani and Castaldi (2014)). By following the same procedure, the second disturbance term representing the $p_d(x)$ function in (2) and due to the wind wakes is described by the term $\hat{C}_{p\,i}$ in (9):

$$\hat{C}_{p\,i}\,(\lambda_j,\,\beta_j) = 0.0027\,\lambda_j^2\,\beta_j - 0.0011\,\lambda_j^2 \qquad (9)$$

with reference to the wind wake from the j–th turbine of the park affecting the i–th turbine.

It is worth noting that the suggested scheme provides the analytical description of the disturbance effects due to all uncertainties, and not only the errors due to C_p entry changes and the wind wake interferences among the wind turbines. However, since these terms are used for the fault estimation filter design, any kind of uncertainty must be modelled. A similar approach was proposed *e.g.* in (Chen and Patton (1999)) but developed only for linear state–space models. Under these considerations, the uncertainty distribution description $p_d(x)$ for the nonlinear model (2) is identified using the input–output data from the wind turbine. The general assumption holding for this case is that the model–reality mismatch is varying more slowly that the disturbance signals, such as d. Another important point regards the fact that the $p_d(x)$ estimation aims at describing the structure of the uncertainty, which should not depend on the wind size uncertainty. Only the so–called directions of the disturbance represent the important effect for disturbance decoupling, *i.e.* the $p_d(x)$ term, and not the 'amplitude' of the uncertainty, *i.e.* the size of the disturbance d.

The designed NLGA adaptive filters (5), (6), and (7), provide the estimate the magnitude of the different faults acting on the the wind farm benchmark, as shown in Section 2. The design of the filter for the compensation of the control fault is sketched in the following. More mathematical details of the general design procedure can be found in (Simani and Castaldi (2014)).

With reference to the input–affine model (2), $x = [x_1\,x_2]^T = [\omega_{i\,g}\,P_{i\,g}]^T$, $c = [P_{i\,r}\,\beta_i]^T$, and:

$$n(x) = \begin{bmatrix} -\dfrac{\rho\,A}{2\,J}\,0.0010\,R^3\,x_1^2 - \dfrac{1}{J}\,x_2 \\ -p_{gen}\,x_2 \end{bmatrix} \qquad (10)$$

$$g(x) = \begin{bmatrix} 0 & \dfrac{\rho\,A}{2\,J}\,0.0003\,R^3\,x_2^2 \\ p_{gen} & 0 \end{bmatrix} \qquad (11)$$

and:

$$\ell(x) = \begin{bmatrix} 0 & \dfrac{\rho\,A}{2\,J}\,0.0003\,R^3\,x_1^2 \\ 0 & 0.0001 \end{bmatrix} \qquad (12)$$

with reference to the i–th turbine, with the understanding that the subscript i is dropped. Moreover, $p_d(x)$ is defined as:

$$p_d(x) = \begin{bmatrix} \dfrac{\rho\,A}{2\,J}\,0.0010\,R^2\,x_1 & 0.0011 \\ 0.0002 & \dfrac{\rho\,A}{2\,J}\,0.0027\,x_2 \end{bmatrix} \qquad (13)$$

In the case of the model (1), with reference to (2), and recalling (13), (12), and (11), it results that:

$$S_0 = \bar{P} = \mathrm{cl}\,(p_d(x)) \equiv p_d(x) \qquad (14)$$

If $\ker\{dh\} = \emptyset$, it follows that $\Sigma_*^P = \bar{P}$ as $\bar{S}_0 \cap \ker\{dh\} = \emptyset$. On the other hand, it is necessary to compute the expression $\left(\Sigma_*^P\right)^\perp = \left(\bar{P}\right)^\perp$. However, it is worth noting that, for the case under investigation, the determination of the codistribution $\left(\Sigma_*^P\right)^\perp = \left(\bar{P}\right)^\perp$ is enhanced due to the structure of (14). Other mathematical details are similar to the derivation of the filters shown in (Simani and Castaldi (2014)), and they will not be reported here.

Finally, the design of the NLGA adaptive filter for the reconstruction of the fault f affecting for example the actuator $\beta_i(t)$ (fault case 2) is based on the expression (15):

$$\dot{\tilde{y}}_{1s} = M_1 \cdot f + M_2 \qquad (15)$$

where:

$$\begin{cases} M_1 = 0.8\,x_1^2 - 0.036\,x_1 \\ M_2 = 1.02\,x_2^2 + 15.7\,x_2 - 0.3\,x_1^3 + 0.77\,x_1^2 \end{cases} \qquad (16)$$

The design of the NLGA adaptive filters for the reconstruction of the faults for the cases 1 and 3 is based on a different selection of the vector of (12), which will lead to other expressions for the filter (15). As an example, for the fault case 2 of Table 1, the nonlinear filter for the reconstruction of f decoupled from the disturbance d representing the effect of both the wind $v_w(t)$ and the wake $v_{w,\,m}$ signals has the form (5). After a suitable choice of the parameters in (5), (6), and (7), the nonlinear filter provided an accurate estimate of the fault size, with minimal detection delay.

Thus, the tests shown below refer to the simulation of the actuator fault f modelled as a sequence of rectangular pulses with random amplitude and length. In particular, Fig. 3 shows the fault estimate $\hat{f}$ (dotted grey line), when compared with the simulated one (dashed black line).

Under this condition, Fig. 4 shows the power reference signal P_r (continuous black line) compared with its desired value (grey dotted line), with fault accommodation.

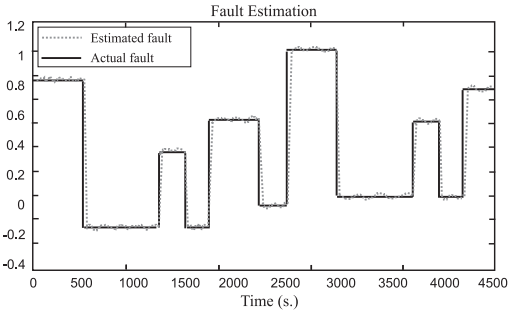

Fig. 3. Real–time estimate $\hat{f}$ of the intermittent fault case 2.

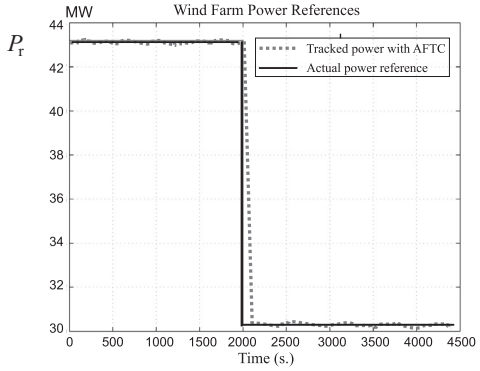

Fig. 4. P_r reference signal for the fault case 2 with AFTCS.

In particular, Fig. 4 depicts the power reference to the wind farm, P_r, which is constant and equal to 43.6MW until $t = 2000$ s, when it changes to about 30 MW. It is worth observing that the suggested NLGA adaptive filter not only provided the fault detection, but also the fault estimate. Moreover, a fault modelled as a sequence of pulses with variable amplitude and length has been considered, since it represent the realistic fault condition in connection with the wind turbine model. However, as already remarked, the fault estimation module can be easily generalised to estimate, for example, polynomial functions of time, or generic signals belonging to a given class of faults, if the NLGA adaptive filters contain the internal model of the fault itself.

In order to summarise the advantages of the proposed strategy, the performance of the AFTCS applied to the wind farm benchmark was evaluated in terms of per–cent Normalised Sum of Squared tracking Error ($NSSE$) and considering different data sequences. Therefore, the simulations were performed by exploiting the wind park simulator, followed by a Matlab® Monte–Carlo analysis. Under this assumption, Table 3 reports the nominal values of the considered wind turbine model parameters with respect to their simulated uncertainty. The Monte–Carlo analysis has been performed by modelling these variables as Gaussian stochastic processes, with zero–mean and standard deviations corresponding to realistic minimal and maximal error values of Table 3.

It was also assumed that the input–output signals u and y and the power coefficient map C_p entries were affected by errors, expressed as per–cent standard deviations of the corresponding nominal values u_0, y_0, and $C_{p\,0}$ also reported in Table 3.

Table 3. Simulated wind farm parameter uncertainties.

Variable	Nominal Value	Min. Error	Max. Error
ρ	1.225 kg/m^3	± 0.1%	± 5%
J	7.794×10^6 kg m^2	± 0.1%	± 25%
C_p	$C_{p\,0}$	± 0.1%	± 20%
u	u_0	± 0.1%	± 25%
y	y_0	± 0.1%	± 25%

Therefore, for performance evaluation of the control schemes, the best, average, and worst values of the $NSSE\%$ index were computed, and experimentally evaluated with 500 Monte–Carlo runs. The value of $NSSE\%$ is computed for several possible combinations of the parameter values reported in Table 3. It is worth noting that Table 3 describes the uncertain parameters that have been simulated in order to analyse the robustness and the reliability of the proposed AFTCS with respect to parameter variations. In fact, the disturbance decoupling approach was proposed for removing the effect of the uncertain wind and wake effects, and not for handling the parameter variations in Table 3.

Table 4 summarises the results obtained by considering the proposed AFTCS integrating the original wind turbine farm for the different fault cases.

Table 4. Comparison of the achievable performance in terms of $NSSE\%$ with respect to different AFTCS and the fault cases.

AFTCS method/Fault	Case 1	Case 2	Case 3
AFTCS with wind and wake decoupling	10.33%	11.56%	10.47%
AFTCS only with wind decoupling (Simani and Farsoni (2018))	14.07%	15.06%	15.34%
PFTCS with fuzzy identification (Simani et al. (2018))	13.74%	14.37%	15.01%

In particular, Table 4 summarises the values of the considered $NSSE\%$ performance index, with reference to the possible combinations of the parameters described in Table 3. The results obtained with the strategy proposed in this paper are also compared with the ones achievable with the approach in (Simani and Castaldi (2014)) with the decoupling of the wind effect, and the fuzzy scheme in (Simani et al. (2018)).

It is worth noting that, regarding the AFTCS method proposed in this paper, Table 4 highlights how this scheme seems to achieve better performances in terms of tracking error with respect to the two other methodologies. Further work will investigate the stability feature of the proposed approach, when applied also to real wind parks.

5. CONCLUSION

This paper addressed the design of an active fault tolerant control scheme applied to a small wind park benchmark. The controller accommodation scheme exploited the on–line estimate of the fault signals generated by nonlinear filters obtained via the nonlinear geometric approach, which is used to obtain important decoupling properties. A data–driven approach was also proposed to provide an analytical formulation of the disturbance effects, which were subsequently used for designing the nonlinear filters for fault

estimation. These features can represent key issues when on–line implementations are used for a viable application of the proposed scheme. A realistic wind farm benchmark was considered to validate the performances of the suggested scheme, in the presence of both modelling and measurement errors. Finally, further investigations will be carried out to evaluate the effectiveness of the suggested approach when applied to real wind farm installations, as well as its analytical stability and robustness properties.

REFERENCES

Baldi, P., Blanke, M., Castaldi, P., Mimmo, N., and Simani, S. (2018). Fault diagnosis for satellite sensors and actuators using nonlinear geometric approach and adaptive observers. *International Journal of Robust and Nonlinear Control*, 2018, 1–27. DOI: 10.1002/rnc.4083.

Castaldi, P., Geri, W., Bonfè, M., Simani, S., and Benini, M. (2010). Design of residual generators and adaptive filters for the FDI of aircraft model sensors. *Control Engineering Practice*, 18(5), 449–459. ACA'07 – 17th IFAC Symposium on Automatic Control in Aerospace Special Issue. Publisher: Elsevier Science. ISSN: 0967–0661. DOI: 10.1016/j.conengprac.2008.11.006.

Castaldi, P., Mimmo, N., and Simani, S. (2017). Avionic Air Data Sensors Fault Detection and Isolation by means of Singular Perturbation and Geometric Approach. *Sensors*, 17(10), 1–19. Invited paper for the special issue "Models, Systems and Applications for Sensors in Cyber Physical Systems". DOI: 10.3390/s17102202.

Chen, J. and Patton, R.J. (1999). *Robust Model–Based Fault Diagnosis for Dynamic Systems*. Kluwer Academic Publishers, Boston, MA, USA.

Odgaard, P.F. and Stoustrup, J. (2012). Fault Tolerant Control of Wind Turbines using Unknown Input Observers. In C. Verde, C.M. Astorga Zaragoza, and A. Molina (eds.), *Proceedings of the 8th IFAC Symposium on Fault Detection, Supervision and Safety of Technical Processes – SAFEPROCESS 2012*, volume 8, 313–319. National Autonomous University of Mexico, Mexico City, Mexico. DOI: 10.3182/20120829-3-MX-2028.00010.

Odgaard, P.F. and Stoustrup, J. (2013). Fault Tolerant Wind Farm Control – a Benchmark Model. In *Proceedings of the IEEE Multiconference on Systems and Control – MSC2013*, 1–6. Hyderabad, India.

Simani, S. and Castaldi, P. (2017). Robust Control Examples Applied to a Wind Turbine Simulated Model. *Applied Sciences*, 8(29), 1–28. DOI: 10.3390/app8010029. Invited paper for the special issue "Renewable Energy 2018".

Simani, S. and Castaldi, P. (2018). Adaptive Robust Control and its Applications. In A.T. Le (ed.), *Robust Control Applications to a Wind Turbine Simulated System*, chapter 11, 217–233. InTech, Rijeka, Croatia. ISBN: 978-953-51-5729-8. DOI: 10.5772/intechopen.71526.

Simani, S. and Farsoni, S. (2018). *Fault Diagnosis and Sustainable Control of Wind Turbines: Robust data–driven and model–based strategies*. Mechanical Engineering. Butterworth–Heinemann – Elsevier, Oxford (UK), 1st edition. ISBN: 9780128129845.

Simani, S., Farsoni, S., and Castaldi, P. (2018). Data–Driven Techniques for the Fault Diagnosis of a Wind Turbine Benchmark. *International Journal of Applied Mathematics and Computer Science – AMCS*, 28(2), 1–13.

Simani, S. and Castaldi, P. (2014). Active Actuator Fault Tolerant Control of a Wind Turbine Benchmark Model. *International Journal of Robust and Nonlinear Control*, 24(8–9), 1283–1303. John Wiley. DOI: 10.1002/rnc.2993.